The cytochrome P450 enzyme CYP24A1 increases proliferation of mutant KRAS-dependent lung adenocarcinoma independent of its catalytic activity

Received for publication, November 12, 2019, and in revised form, March 5, 2020 Published, Papers in Press, March 12, 2020, DOI 10.1074/jbc.RA119.011869

Wei Huang[‡1], Paramita Ray[§1], Wenbin Ji[§2], Zhuwen Wang[¶], Derek Nancarrow[¶], Guoan Chen[¶3], Stefanie Galbán[‖], Theodore S. Lawrence[§], David G. Beer[§¶], Alnawaz Rehemtulla[§], Nithya Ramnath[‡4], and Dipankar Ray[§5]**

*From the [§]Departments of Radiation Oncology, [‡]Internal Medicine, [¶]Surgery, and [‖]Radiology, University of Michigan Medical School, Ann Arbor, Michigan 48109 and **Veterans Administration, Ann Arbor Healthcare System, Ann Arbor, Michigan 48105*

Edited by Alex Toker

We previously reported that overexpression of cytochrome P450 family 24 subfamily A member 1 (CYP24A1) increases lung cancer cell proliferation by activating RAS signaling and that CYP24A1 knockdown inhibits tumor growth. However, the mechanism of CYP24A1-mediated cancer cell proliferation remains unclear. Here, we conducted cell synchronization and biochemical experiments in lung adenocarcinoma cells, revealing a link between CYP24A1 and anaphase-promoting complex (APC), a key cell cycle regulator. We demonstrate that CYP24A1 expression is cell cycle–dependent; it was higher in the G_2-M phase and diminished upon G_1 entry. CYP24A1 has a functional destruction box (D-box) motif that allows binding with two APC adaptors, CDC20-homologue 1 (CDH1) and cell division cycle 20 (CDC20). Unlike other APC substrates, however, CYP24A1 acted as a pseudo-substrate, inhibiting CDH1 activity and promoting mitotic progression. Conversely, overexpression of a CYP24A1 D-box mutant compromised CDH1 binding, allowing CDH1 hyperactivation, thereby hastening degradation of its substrates cyclin B1 and CDC20, and accumulation of the CDC20 substrate p21, prolonging mitotic exit. These activities also occurred with a CYP24A1 isoform 2 lacking the catalytic cysteine (Cys-462), suggesting that CYP24A1's oncogenic potential is independent of its catalytic activity. CYP24A1 degradation reduced clonogenic survival of mutant *KRAS*-driven lung cancer cells, and calcitriol treatment increased CYP24A1 levels and tumor burden in *Lsl-KRAS^{G12D}* mice. These results disclose a catalytic activity-independent growth-promoting role of CYP24A1 in mutant *KRAS*-driven lung cancer. This suggests that CYP24A1 could be therapeutically targeted in lung cancers in which its expression is high.

Barely 35% of patients with metastatic lung cancer survive 1 year after diagnosis using modern chemoimmunotherapy regimens (1). Increased understanding of the molecular biology of lung cancer has led to the identification of specific oncogenic drivers that have been successfully targeted to improve the survival of a small minority of patients (*e.g.* those driven by *EGFR* mutations, *ALK* or *ROS1* rearrangements) (2, 3). However, for the majority of tumors, the genetic drivers are still poorly defined with limited treatment options. *CYP24A1* is a member of the cytochrome P450 superfamily of enzymes that encodes for 24-hydroxylase, which catabolizes 1,25-D_3, the biologically active form of vitamin D (4). *CYP24A1* is overexpressed at baseline in numerous cancers (compared with surrounding normal), including breast (associated with amplification) and esophageal cancers (5, 6). We earlier reported a correlation between *CYP24A1* in lung adenocarcinoma and survival; the probability of survival at 5 years was 42% (in patients with high *CYP24A1*, $n = 29$) *versus* 81% (low *CYP24A1*, $n = 57$) ($p = 0.007$) (7). In the same study, a validation set of 101 lung adenocarcinomas confirmed that *CYP24A1* was independently prognostic of poor survival. We also reported that overexpression of CYP24A1 promotes lung cancer cell proliferation and invasion, whereas, knockdown reduces tumor growth (8). Similarly, various inducers of CYP24A1 expression, such as bile salts, cigarette smoke etc., are known to increase cell proliferation. Besides CYP24A1, few other cytochrome P450 family members (*e.g.* CYP1A1, 11A1) are also reported to induce cell proliferation (9, 10). However, the molecular regulators involved in CYP-mediated regulation of cell proliferation is yet unclear.

Several cell cycle regulators, particularly the cyclins, contain consensus amino acid sequence (R*XXL*X*XX*N/D/E, where *X* could be any amino acid) termed the destruction box, or D-box. This sequence is recognized by a multisubunit ubiquitin ligase (E3) complex called the anaphase-promoting complex or cyclosome (APC/C).[6] APC is primarily responsible for ubiquitin-

This work was supported by NCI, National Institutes of Health Grant R01CA160981 (to D. R.) and Veterans Administration Merit Award I01CX000333-02 (to N. R.). The authors declare that they have no conflicts of interest with the contents of this article. The content is solely the responsibility of the authors and does not necessarily represent the official views of the National Institutes of Health.

This article contains Figs. S1 and S2.

[1] These authors contributed equally to this work.

[2] Present address: Arbor Research Collaborative for Health, Ann Arbor, MI 48105.

[3] Present address: School of Medicine, Southern University of Science and Technology, Shenzhen, China 518055.

[4] To whom correspondence may be addressed: 1500 East Medical Center Dr., Ann Arbor, MI 48109. Tel.: 734-845-5800; E-mail: nithyar@umich.edu.

[5] To whom correspondence may be addressed: Medical Science Bldg. I, Ann Arbor, MI 48109-2026. Tel.: 734-936-9162; Fax: 734-763-1581; E-mail: dipray@umich.edu.

[6] The abbreviations used are: APC/C, anaphase-promoting complex or cyclosome; D#1, ^{98}RMKLGSFE^{105}; D#2, ^{223}RFGLLQKN^{230}; AC, adenocarcinoma.

mediated proteasomal degradation of several cell cycle regulators (11, 12), including cyclins, various CDK regulators and even other ubiquitin ligases (13), thus intricately orchestrating the regulation of nuclear division. Such regulated proteolysis triggers the progression of various phases of cell cycle (14). Importantly, the ubiquitin ligase activity of APC/C is regulated in a cell cycle oscillating fashion by phosphorylation and by sequential recruitment of two activators of WD40-repeat proteins called CDH1 (or HCT1) and CDC20 (or Fizzy) (15). An additional layer of APC/C activity regulation is achieved by the binding of pseudo-substrates (such as EMI1, ACM1, MAD3, etc.) that competitively inhibit APC/C substrate binding utilizing their own D-boxes (16–18). Although CYP24A1 has been recognized as an oncogene in multiple cancer types, all targeting efforts have been focused on modulating enzymatic activity. The thought was that inhibiting the catalytic activity of CYP24A1 would increase the concentration of its key substrate Vitamin D and this would lead to anti-tumor effects. Studies testing nonselective CYP catalytic inhibitor (ketoconazole) demonstrated limited benefit (19). Herein, we report an enzymatic activity independent role of CYP24A1 in lung cancer progression. Specifically, we discovered that the CYP24A1 putative D-box motifs function to potently inhibit the ubiquitin ligase activity of APC-CDH1, a well-documented tumor suppressor. We describe experiments that establish the importance of the physical presence (as opposed to the catalytic activity) of CYP24A1 in lung cancer progression that can inform strategies to physically abolish CYP24A1. Additionally, such information may provide insights about the possible oncogenic properties of other CYP family members, many of which have similar D-boxes.

Results

CYP24A1 expression is cell cycle regulated

Cytochrome P450 is a large family of 57 genes with over 1000 alternately spliced transcript variants, all of which have been primarily studied to understand their roles in various drug and xenobiotics metabolism (20). We previously reported that CYP24A1 overexpression enhances lung cancer cell proliferation (8) and also associated with poorer survival in lung adenocarcinoma. However, we had not assessed the relative contribution of catalytic activity on proliferation. *CYP24A1* is predicted to express multiple isoforms. Among those, isoform 1 (Iso1) with 11 exons is the full-length (514 amino acids) and the most abundant isoform with vitamin D catalytic activity. An alternate isoform (Iso2) lacks exon 10, encoding heme-binding domain and the catalytic cysteine (Cys-462), thereby unable to catalyze vitamin D. As reported in prostate (21) and colon cancers (22), we too noted Iso2 transcript abundance compared with matched normal tissue in a cohort of 58 lung cancers derived from the TCGA RNA-Seq data (23, 24) (Fig. 1*A*). To understand the impact of isoform-specific overexpression of CYP24A1 on cell proliferation we overexpressed either DDK- or V5-tagged Iso1 and Iso2, respectively, in SK-Lu1 and Hcc827 cells (Fig. 1*B*). Overexpression of CYP24A1 in mutant *KRAS* containing human lung adenocarcinoma, SK-Lu1 cells (with undetectable levels of endogenous CYP24A1), showed increased proliferation compared with vector control assessed using cell counting and MTT assays (Fig. 1*C*). In comparison, Iso2 also showed increased proliferative potential, suggesting that CYP24A1 cell proliferating ability is independent of its catalytic activity. Surprisingly, in Hcc827 cells (WT KRAS), overexpression of CYP24A1 (either Iso1 or Iso2) reduced proliferation rates, suggesting a cooperativity between mutant KRAS and CYP24A1 (Fig. 1*D*).

To determine whether CYP24A1 has any direct role in cell cycle, we examined the levels of endogenous CYP24A1 protein in HeLa cells synchronized by double thymidine block and release (Fig. 1*E*), a validated model for such studies. The expression of CYP24A1 was highest 8–10 h after release and decreased promptly by 12 h, which closely matched the expression pattern of mitotic cyclin B1 expression (Fig. 1*F*). As there are no isoform-specific CYP24A1 antibodies currently available, we performed synchronization and release experiments in SK-Lu1 cells (a lung adenocarcinoma cell line with mutant KRAS and undetected levels of CYP24A1) stably expressing V5-tagged Iso2. Using V5 antibody, we observed increases in CYP24A1 protein at 4 and 14 h following double thymidine block and release, which again mirrored cyclin B1 expression (Fig. 1*G*). Cellular DNA content analyzed using fluorescence-activated cell sorting (FACS) revealed that the cells expressing highest Iso2-V5 were in G_2/M phase of the cell cycle and decreased upon exit (Fig. 1*H*). Together, we conclude that CYP24A1 including the Iso2 is a cell cycle–regulated protein that accumulates during G_2/M, subsequently undergoing degradation while exiting mitosis.

CYP24A1 contains D-boxes, critical for APC-CDH1 regulation

As CYP24A1 expression closely overlapped with cell cycle-dependent expression of cyclin B1, we analyzed the amino acid sequence of CYP24A1 and identified two D-boxes (^{98}RMKLGSFE^{105} and ^{223}RFGLLQKN^{230}), hereby referred to as D#1 and D#2, respectively (Fig. 2*A*). Both D-boxes are conserved among vertebrates including human, mouse, rat, and zebrafish. Phylogenetic analyses of cytochrome P450 family members grouped CYP24A1 closer to CYP11A1, 1A1, and 17A1 family members with previously reported roles in cell proliferation (Fig. 2*B*). Primary amino acid sequence analysis further revealed the presence of D-boxes (Fig. 2*B*) in the aforementioned members as well as in few others (2A6, 21A2, etc.), which supports a common mechanistic involvement in cell cycle regulation using a common regulatory domain (D-box).

To understand the functional importance of D-boxes in CYP24A1, we performed immunoprecipitation analysis using the V5 antibody and noted stable interactions of CYP24A1-Iso2 with both APC/C^{CDH1} and APC/C^{CDC20} (Fig. 2, *C* and *D*). Mutation of Arg-98 and Lys-101 of the D#1 to alanine (A) had no impact on CYP24A1–CDH1 interaction (Fig. 2*C*, *lanes 4* and *5*). While analyzing the catalogue of somatic mutations in cancer (COSMIC) database, we identified mutations at Arg-223 and Lys-226 positions of D#2. We, therefore, mutated both Arg-223 and Lys-226 to alanine (A) and tested the mutant CYP24A1 interaction with APC/C, where we noted reduced interaction with the D#2 mutant, demonstrating the importance of CYP24A1 D#2 (Fig. 2*D*, *lanes 5–7*). D-box– containing

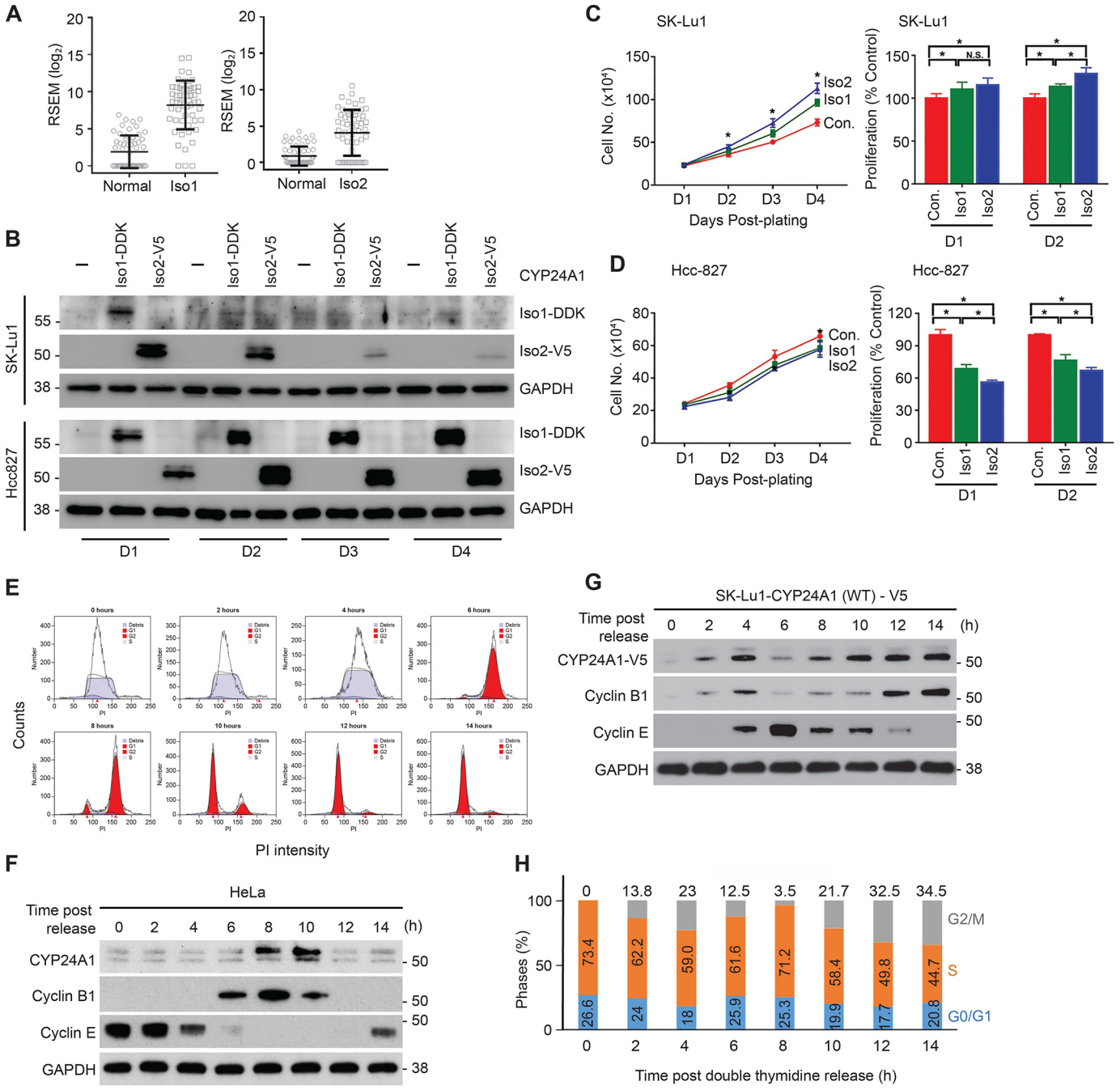

Figure 1. CYP24A1 is a cell cycle–regulated protein involved in cell proliferation independent of its catabolic activity. *A*, CYP24A1 expression data from TCGA matched paired lung tissue RNA-Seq cohort ($n = 58$) of lung adenocarcinoma patients showing higher expressions of both Iso1 and Iso2 in the tumor tissue compared with normal lung. *B*, immunoblotting using specified antibodies showing overexpression of CYP24A1 Iso1 construct tagged with DDK and Iso2 construct tagged with V5 on different days (D1–D4) post irradiation in SK-Lu1 and Hcc827 cells. *C* and *D*, cell counting (*left panels*) and MTS assay (*right panels*) in SK-Lu1 (in *C*) and Hcc827 (in *D*) cells showing increased proliferation upon overexpression of both Iso1 and Iso2 in SK-Lu1 cells, however, similar studies in Hcc827 cells shows growth delay. *E*, HeLa cells were synchronized using double thymidine block and released. *E* and *F*, cells and cell lysates were collected at the indicated times and were subjected to either FACS (in *E*) or immunoblotting (in *F*). *G* and *H*, SK-Lu1 cells stably expressing CYP24A1-Iso2-V5 protein were synchronized and released and cell lysates were subjected to immunoblotting using indicated antibodies and assessed for cell cycle distribution (in *H*).

proteins appear to be either substrates (able to bind and be ubiquitinated and degraded by APC) or pseudo-substrates (able to bind but not be ubiquitinated and degraded by APC; however, this binding competitively blocks the degradation of other CDH1 substrates). We tested the steady state levels of WT CYP24A1 protein in the presence and absence of CDH1. A dose-dependent increase of CDH1 failed to down-regulate CYP24A1-Iso2; instead, an increase in steady state level was noted, suggesting it may not be a true APC/C substrate (Fig. 2*E*). Using *in vivo* ubiquitination assay using CDC20 as a CDH1 substrate (25), we discovered that CYP24A1-WT overexpression inhibits CDH1-mediated CDC20 polyubiquitination, whereas, D#2 mutant overexpression resulted in CDC20 hyper-polyubiquitination (Fig. 2*F*). Using an *in vitro* ubiquitination

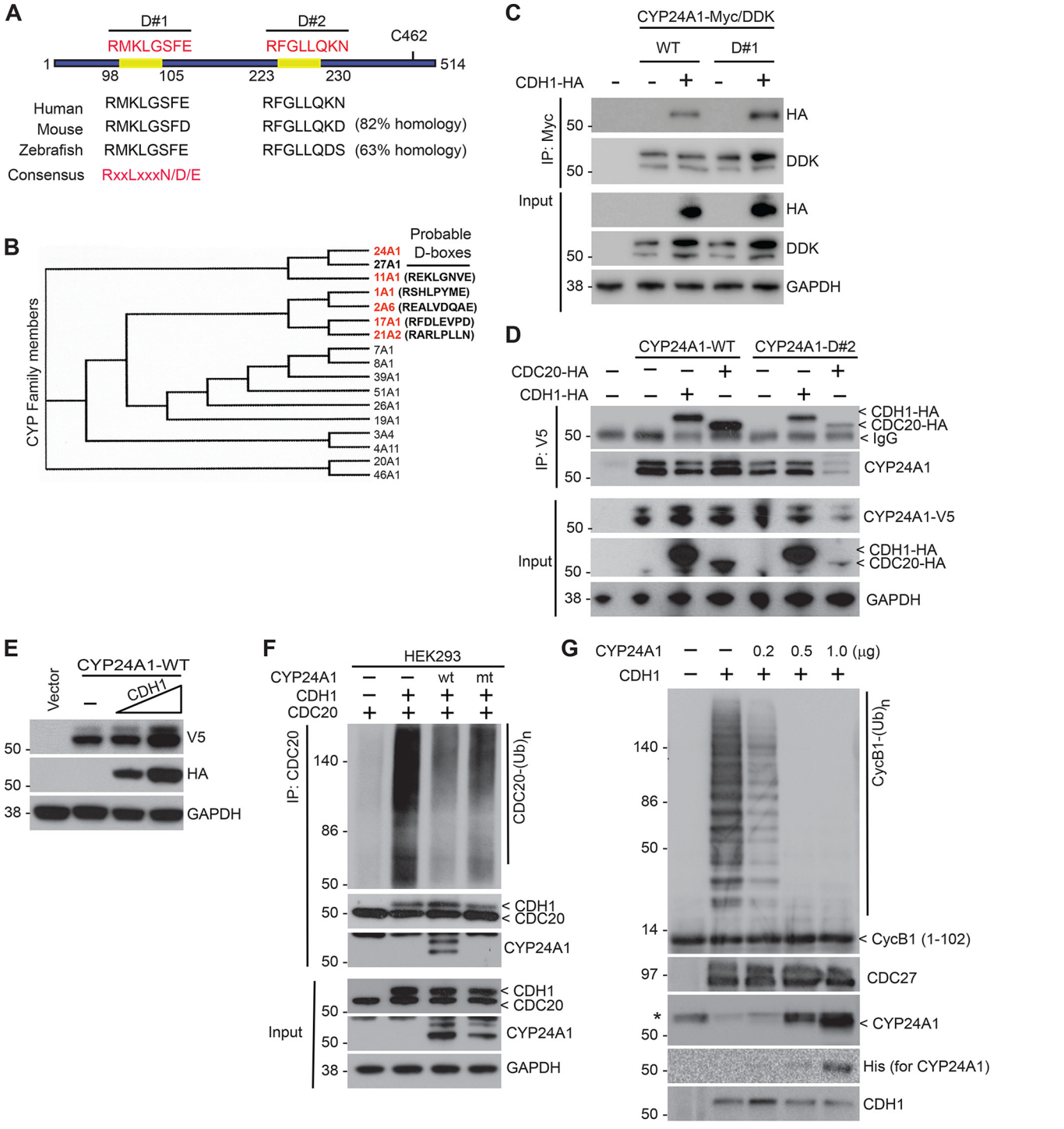
A
D#1
RMKLGSFE
D#2
RFGLLQKN
C462
1
98
105
223
230
514
Human RMKLGSFE RFGLLQKN
Mouse RMKLGSFD RFGLLQKD (82% homology)
Zebrafish RMKLGSFE RFGLLQDS (63% homology)
Consensus RxxLxxxN/D/E
B
Probable D-boxes
CYP Family members
24A1
27A1
11A1 (REKLGNVE)
1A1 (RSHLPYME)
2A6 (REALVDQAE)
17A1 (RFDLEVPD)
21A2 (RARLPLLN)
7A1
8A1
39A1
51A1
26A1
19A1
3A4
4A11
20A1
46A1
C
CYP24A1-Myc/DDK
WT
D#1
CDH1-HA
IP: Myc
HA
DDK
Input
GAPDH
D
CYP24A1-WT
CYP24A1-D#2
CDC20-HA
CDH1-HA
IP: V5
CDH1-HA
CDC20-HA
IgG
CYP24A1
CYP24A1-V5
Input
GAPDH
E
CYP24A1-WT
Vector
CDH1
V5
HA
GAPDH
F
HEK293
CYP24A1
wt
mt
CDH1
CDC20
IP: CDC20
CDC20-(Ub)n
CDH1
CDC20
CYP24A1
Input
GAPDH
G
CYP24A1
0.2
0.5
1.0 (μg)
CDH1
CycB1-(Ub)n
CycB1 (1-102)
CDC27
CYP24A1
His (for CYP24A1)
CDH1
H
CYP24A1-V5 (WT)
CYP24A1-V5 (D#2)
CHX
0 10 20 30 45 60 90 180 360 0 10 20 30 45 60 90 180 360 (min)
V5
GAPDH
I
WT (T1/2 ~60 min)
D#2 (T1/2 ~240 min)
Relative intensity (a.u.)
Time (in mins)

assay where a 1–102 amino acid fragment of cyclin B1 (a known CDH1 substrate) was incubated with APC-CDH1 complex (immunoprecipitated from G_1-synchronized HeLa cells), we noted a robust polyubiquitination of purified cyclin B1 fragment, which was significantly inhibited upon addition of increasing concentrations of recombinant CYP24A1-Iso2 (Fig. 2*G*). Furthermore, the D#2 mutant protein half-life was shorter (~60 min) compared with ~240 min for WT Iso2 protein (Fig. 2, *H* and *I*), suggesting the D#2 box may not be a degradation signal for CYP24A1 but instead acts as a pseudo-substrate to regulate APC^{CDH1} activity. Upon D#2 mutation, loss of its interaction with APC/C contributed to faster decay by a yet unknown E3 ligase.

Overexpression of WT CYP24A1-Iso2 enhances cell proliferation, whereas D#2 box mutant prevents mitotic exit and leads to cell death

As we discovered CYP24A1's ability to inhibit APC/C^{CDH1} ubiquitin ligase activity, we next addressed the effect of CYP24A1 expression on cell cycle progression. For this study, SK-Lu1 cells stably expressing either WT or D#2 mutant were used. The cells were then synchronized using double thymidine block followed by release. As shown in Fig. 3*A*, in all three groups (vector, WT, and D#2 mutant) within 4-h post thymidine release, a significant percentage (35–45%) of cells entered the first round of mitosis. Within 6–8 h post release, although the majority of cells from the vector control and Iso2 WT expressing groups exited mitosis and entered next round of G_1 phase, about 10–15% of SK-Lu1 cells expressing D#2 mutant failed to exit mitosis. Furthermore, cells expressing Iso2 WT entered the second round of mitosis by 12 h post thymidine release (14 h in case of vector transfected SK-Lu1 cells), illustrating the growth promoting potential of WT CYP24A1-Iso2 expression. In contrast, a majority of cells expressing D#2 mutant failed to exit mitosis, and by 14–24 h post thymidine release, a gradual increase (4–10%) of cells with sub-G_1 DNA content were detected using FACS, suggestive of cell death (Fig. 3*B*). Under phase-contrast microscope we have similarly noted death of cells undergoing mitosis (not shown). While analyzing cell lysates (Fig. 3*C*), we noted several differences in SK-Lu1 cells expressing D#2 mutant compared with CYP24A1 WT: (i) diminished cyclin B1 accumulation (ii) diminished CDC20 levels, whereas, (iii) an increased accumulation of p21 was observed. These findings led us to propose a model (Fig. 3*D*) where we hypothesize CYP24A1 acts as a major APC/C^{CDH1} regulator. Reduced interaction between CDH1 and CYP24A1 D#2 mutant allows hyperactivation of CDH1, which in turn degrades cyclin B1 and CDC20, the two established CDH1 substrates. With reduced cyclin B1 accumulation, mitotic progression is possibly hindered. Additionally, reduced CDC20 levels, a ligase responsible for p21 degradation during mitotic exit (26), allows p21 to accumulate in an untimely fashion, resulting in the inability to exit mitosis, and instead promotes cell death via mitotic catastrophe. Together, we demonstrate that CYP24A1 is a key participant in nuclear division.

CYP24A1 degradation reduces clonogenic survival of lung cancer cells, whereas its up-regulation increases tumor burden in Lsl-$Kras^{G12D}$ mouse lung tumor model

As overexpression of CYP24A1-Iso2 (lacking catalytic Cys-462 residue) promotes tumor cell proliferation, and as we previously reported that siRNA/shRNA-mediated loss of CYP24A1 reduces clonogenic survival and inhibits tumor growth of mutant KRAS-containing lung cancer cell lines (8), we hypothesized that agent(s) capable of reducing CYP24A1 levels will promote cancer cell death. Our studies indicated that oncogenicity of CYP24A1 is mediated via increased RAS signaling (8). We therefore tested a combination of MEK inhibitor and statin that has previously been shown to decrease the expression of CYP24A1 (27). Additionally, statins have been shown to overcome MEK inhibitor resistance by suppressing AKT activation in cancer cells (28). We tested the effects of MEK inhibitors alone or in combination with simvastatin on CYP24A1 steady state levels. When human lung adenocarcinoma (NCI-H441) cells overexpressing CYP24A1-Iso2-V5 were treated either with a MEKi (PD98059) or simvastatin, there was minimal impact on CYP24A1 levels. Interestingly, a combination of PD98059 and simvastatin significantly reduced (80% loss) CYP24A1 levels compared with control (Fig. 4, *A* and *C*, and Fig. S1), which was rescued by treating cells with a proteasomal inhibitor, MG132. Consequently, this drug combination reduced the clonogenic survival of this mutant *KRAS*-driven cell line (Fig. 4*B*). Similar results were obtained with another mutant *KRAS*-driven NCI-H727 line (data not shown). In mutant *KRAS*-independent A549 cells, a similar drug combination failed to reduce clonogenic survival (Fig. S2*A*), where we noted higher levels of activated AKT compared with more sensitive NCI-H441 cells (Fig. S2*B*). In a parallel experiment, treatment of mouse pancreatic cell lines carrying doxycycline-inducible mutant $KRAS^{G12D}$ alleles when treated with calcitriol, an active form of vitamin D, enhanced cell proliferation and survival (Fig. 4, *D* and *E*) with concomitant induction of CYP24A1 (Fig. 4*F*). However, in WT *KRAS* containing Hcc827 cells, calcitriol treatment inhibited proliferation and clonogenic survival (Fig. 4, *G* and *H*) with induction of CYP24A1 (Fig. 4*I*). We noted similar outcome upon overexpression of CYP24A1 Iso1 and Iso2 in Hcc827 cells (Fig. 1*D*). Together, we hypothesize that CYP24A1 protein levels may be critical for

Figure 2. CYP24A1 contains D-boxes, critical for APC-CDH1 regulation. *A*, schematics showing the location and sequence of two D-boxes (D#1 and D#2) and the catalytic cysteine (Cys-462) in CYP24A1. Both the D-boxes found to be conserved in vertebrates. *B*, phylogenetic analysis of CYP family members showing presence of D-boxes specifically in CYP24A1-related members (*in red*). *C*, HEK293 cells were transfected with indicated plasmids overexpressing either WT or D#1 mutant. 24 h post transfection, cell lysates were subjected to immunoprecipitation using anti-Myc agarose beads (for CYP24A1 pulldown) and immunoblotted with indicated antibodies. *D*, similar immunoprecipitation (using anti-V5 agarose beads) followed by immunoblotting experiments were performed as above. *E*, in HEK293 cells CYP24A1-WT protein was expressed in the presence of increasing (*incline*) concentrations of CDH1 and 24 h post-transfection cell lysates were immunoblotted with indicated antibodies. *F*, *in vivo* ubiquitination assay using CDC20 (as substrate) and CDH1 (as E3) in the presence and absence of either WT or D#2 mutant (*mt*) of CYP24A1. CYP24A1-WT reduced CDH1-mediated CDC20 polyubiquitination. *G*, *in vitro* ubiquitination assay using recombinant CYP24A1-His protein showing CDH1-mediated inhibition of cyclin B1 polyubiquitination. *H* and *I*, protein half-life of CYP24A1 (either WT or D#2) as determined by treating cells with cycloheximide (50 μg/ml). Data plotted were the mean ± S.E. from three independent experiments.

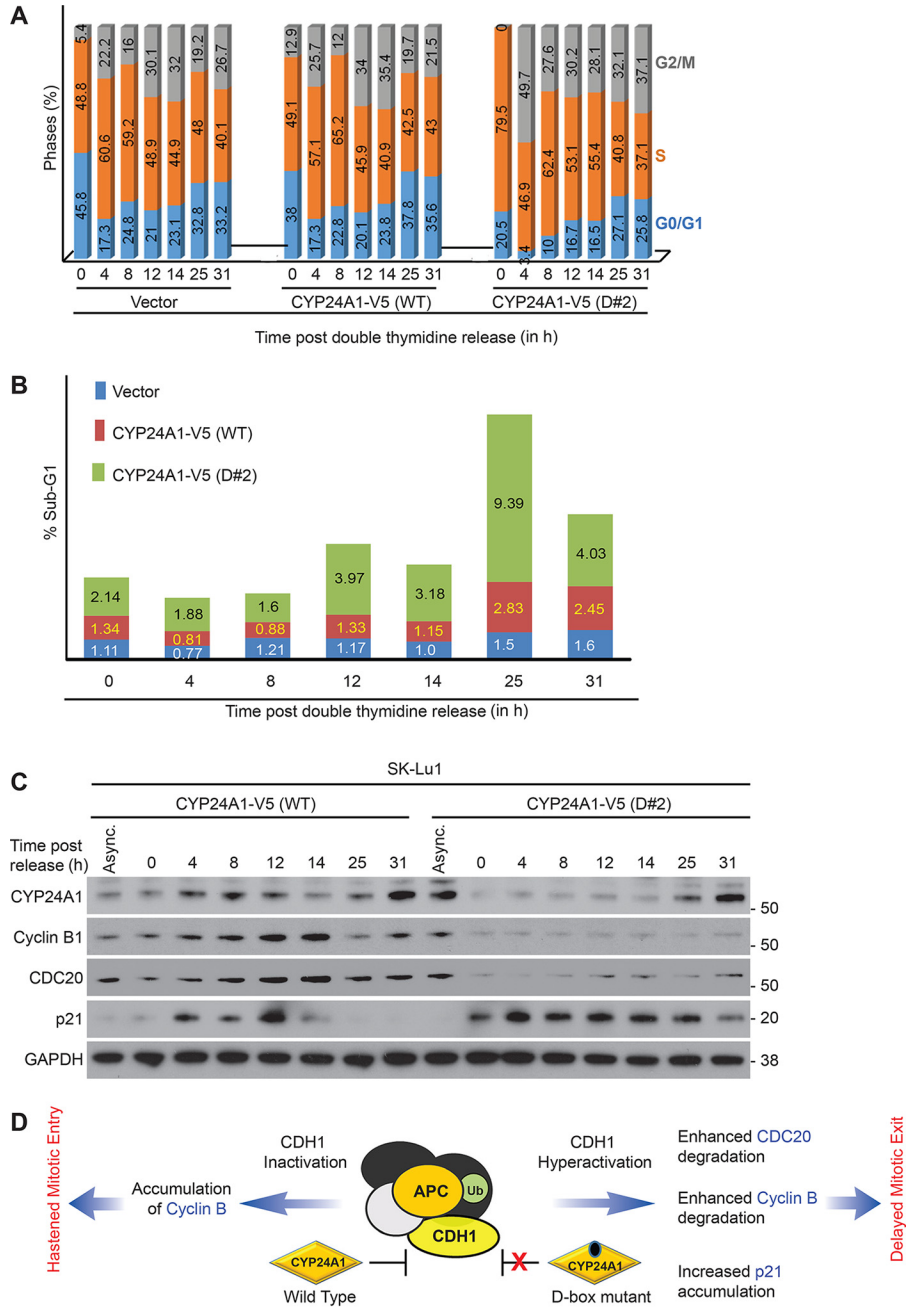

Figure 3. Overexpression of WT CYP24A1-Iso2 enhances cell proliferation, whereas D#2 box mutant prevents mitotic exit and leads to cell death. *A*, SK-Lu1 cells stably transfected either with vector control or CYP24A1 (WT and D#2 mutant) were synchronized with double thymidine block and released. FACS data showing percentage of cells at different phases of cell cycle at different time points. *B*, FACS data showing increased sub-G_1 (possibly mitotic catastrophe) percentage in D#2 overexpressing cells, which may be correlated with mitotic arrest (FACS data in *panel A*). *C*, cell lysates isolated from CYP24A1-WT and D#2 mutants were subjected to immunoblotting using indicated antibodies. *D*, schematic model showing CDH1 hyperactivation in D#2 mutant overexpressing cells leading to reduced cyclin B and CDC20 levels and increased p21 accumulation resulting in delay in mitotic exit causing mitotic catastrophe.

tumor cell proliferation, where mutant *KRAS* dependence may be critical. To test such a hypothesis *in vivo*, we used *lox-STOP-lox-Kras*^{G12D} mouse lung cancer model (29) where tissue- and/or time-dependent expression of Cre recombinase removes the STOP cassette and allows expression of the mutated *Kras* allele. Intranasal infection with an adenovirus encoding Cre results in a high frequency of lung tumors within 18–20 weeks post infection. To study tumor growth noninvasively, we crossed this mouse with an *Lsl-Rosa26-Luciferase* mouse to generate a compound transgenic model, where *Kras*^{G12D} transcription coincides with Luciferase expression in a tissue-specific manner (30). In that study we demonstrated that bioluminescence imaging is sensitive in detecting tumor burden as early as week 13 post Adeno-Cre expression, which correlated with micro-CT imaging captured at week 18. To induce CYP24A1, calcitriol (0.625 μg/kg, i.p. every other day) was injected starting 48 h post Adeno-Cre infection. Tumor development was monitored noninvasively using bioluminescence imaging. As shown in Fig. 5*A*, bioluminescence (-fold change) was 2 fold higher in calcitriol-treated group compared with

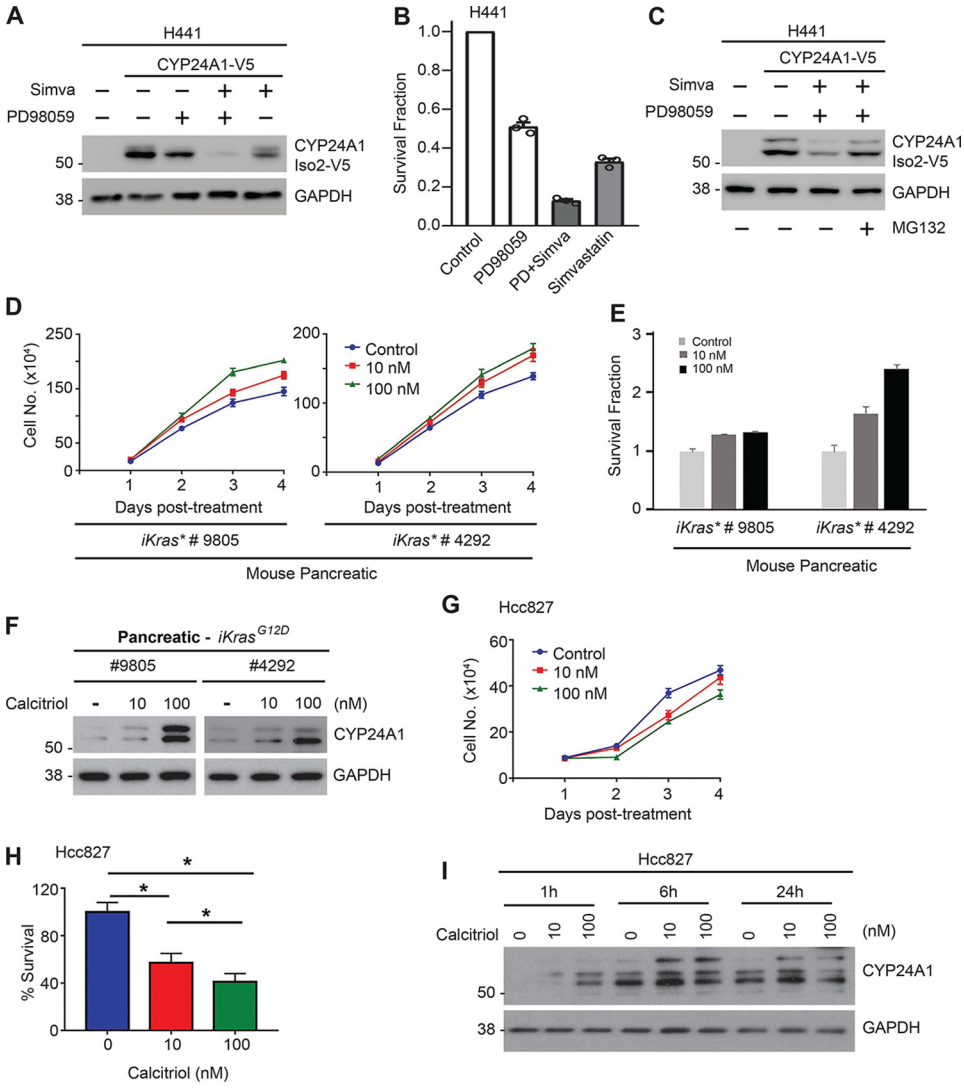

Figure 4. Alteration of CYP24A1 levels differentially impacts the clonogenic survival of lung cancer cells based on mutant KRAS dependence. *A* and *B*, H441 cells overexpressing CYP24A1-Iso2-V5 were treated either with PD98059 (20 μM), simvastatin (20 μM), or in combination showing significant down-regulation of CYP24A1 in combination treatment, which was correlated with the clonogenic survival as shown in (*B*). *C*, CYP24A1-Iso2-V5 overexpressing H441 cells were treated with a combination of simvastatin and PD98059 compounds as above for 20 h followed by a treatment with MG132 (2 μM for the last 4 h), where indicated. Cell lysates were then subjected to immunoblotting using indicated antibodies. *D* and *E*, mouse pancreatic adenocarcinoma cell lines (9805 and 4292) with doxycycline-inducible mutant $KRAS^{G12D}$ expressing cassette (*iKras**) were treated either with vehicle or with different concentrations (10 and 100 nM) of calcitriol. Cell numbers were counted on different days post calcitriol treatment as indicated (in *D*) and clonogenic survival was assayed (in *E*) as described in methods section. *F*, immunoblotting of cell lysates isolated from the above two mouse *iKras** cell lines treated with calcitriol showing induction of CYP24A1. *G* and *H*, effect of calcitriol on cell proliferation and clonogenic survival in WT KRAS containing Hcc827 cells showing growth inhibitor effects. *I*, CYP24A1 induction was noted in Hcc827 cells upon calcitriol treatment in a dose- and time-dependent manner.

vehicle control ($n = 4$ per group). Similar increase in tumor burden was observed in calcitriol-treated group when mice were subjected to micro-CT imaging (Fig. 5*B*). At the completion of study after 20 weeks post virus infection, H&E staining confirmed bioluminescence imaging and micro-CT findings (Fig. 5*C*). Tumor cell lysates isolated 2 weeks post calcitriol treatment showed compensatory up-regulation of CYP24A1 compared with vehicle control (Fig. 5*D*). Together, we show that in $Lsl\text{-}Kras^{G12D}$ mice calcitriol treatment induces CYP24A1 to enhance tumor growth.

Discussion

Here, we provide a novel molecular insight pointing to a direct role of CYP24A1 in cell cycle regulation. Although a few cytochrome P450 family members including CYP24A1 have been implicated in cell cycle regulation, underlying mechanisms have not been clearly addressed. Rodriguez and Potter (9) showed that CYP1A1 can regulate breast cancer cell proliferation by regulating AMP kinase phosphorylation; similarly, the Toyoshima group (10) has shown an indirect involvement of CYP11A1 and CYP17A1 in the regulation of centriole cohesion during mitosis by regulating the synthesis of pregnenolone (P4) and 17 OH-pregnenolone (P5), respectively, from cholesterol. Here, with the identification of a D-box (D#2) in CYP24A1 we found that such a domain allows binding with two of the APC adaptor proteins, CDH1 and CDC20. However, unlike a typical APC substrate, which upon binding undergoes polyubiquitination and degradation, CYP24A1 is recognized as a pseudo-sub-

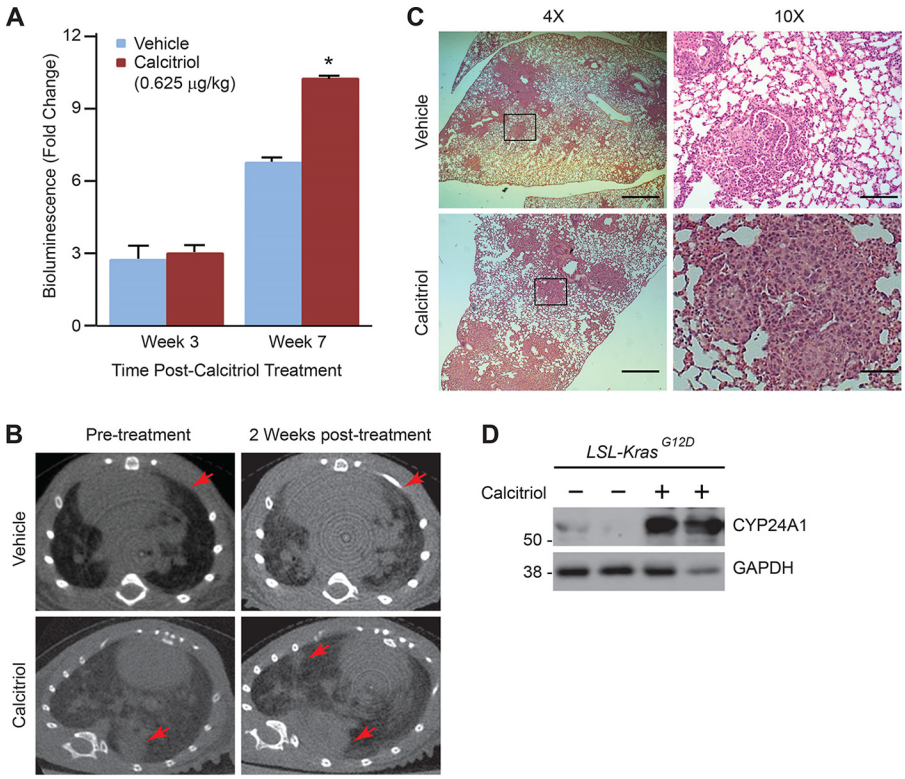

Figure 5. Calcitriol treatment up-regulates CYP24A1 levels and increases tumor burden in *Lsl-Kras^{G12D}* mouse lung tumor model. *A*, follow up of tumor progression using noninvasive bioluminescence -fold change in *LSL-KrasG12D/+; LSL-Rosa26-Luc/+* tumor-bearing mice after 3 and 7 weeks post calcitriol (0.625 mg/kg, i.p., every other day) compared with vehicle-treated mice ($n = 4$ mice per group). *B*, similar groups of mice were imaged using micro CT, either prior to (*left panels*) or 2 weeks post calcitriol treatments. Increase in tumor volume and multiplicity were visible in calcitriol-treated group. *C*, representative H&E-stained sections at 4× (*scale bar*, 500 μm) and 10× (*scale bar*, 200 μm) magnifications of *LSL-Kras^{G12D}* mice lungs treated with vehicle (*top*) and calcitriol (*bottom*). *D*, representative immunoblot showing CYP24A1 up-regulation in calcitriol-treated transgenic mice compared with vehicle control.

strate to inhibit APC^{CDH1} activity similar to Emi1 (16) and Acm1 (31). As reported in other cases, CDH1-mediated polyubiquitination and degradation is determined by its affinity for its substrates (14). Whether such a premise explains how CYP24A1 behaves as a pseudo-substrate and whether additional domains (such as a putative ABBA motif (32)) may be determining CYP24A1 affinity toward APC^{CDH1} remains to be tested. Interestingly, our identification of D-boxes in phylogenetically related cytochrome P450 family members including CYP1A1, 11A1, and 17A1 with known involvement in cell cycle regulation is novel. Future studies may decipher the existence of a conserved pathway among a few cytochrome P450 family members that allow crosstalk between cellular metabolism and cell proliferation. Indeed, the catalytic activity–mediated regulation of various biological processes by cytochrome P450 family members has remained the primary focus of research in the field. Our identification of D-boxes in CYP24A1 and further mutational analyses revealed that the cell cycle regulatory function of CYP24A1 may be independent of its vitamin D catalytic activity. Clinical trials (breast (NCT00212095) and prostate (NCT00536991)) that attempted to target enzymatic activity of CYP24A1 (to increase its substrate calcitriol) using nonspecific inhibitors such as ketoconazole, have not been successful and have not led to use in the clinic. In contrast, we and others have reported that siRNA/shRNA-mediated knockdown of *CYP24A1* provides a more potent and durable anti-proliferative effect, suggesting that the physical presence of CYP24A1 may be critical for tumor cell proliferation and oncogenesis (8, 33).

Our study in *KRAS* mutant lung adenocarcinoma (AC) was based on our previous work as well as by others that suggested that *KRAS* mutant lung AC was associated with higher CYP24A1 expression (22, 35). Others have recently reported that RAF signaling can be attenuated by inhibiting CYP24A1 (36, 37) and in an independent study B-RAF was reported to be a CDH1 substrate interacting via its D-box (D#4) to regulate B-RAF abundance (38). To our surprise, we noted that a combination treatment of MEKi and simvastatin promotes CYP24A1 proteasomal degradation to reduce clonogenic survival of mutant *KRAS*-driven lung cancer cells (Fig. 4*B*). Furthermore, based on reports that statins can overcome the MEKi resistance (28), we too demonstrated a synergistic effect on cell proliferation using combination of MEKi and simvastatin in a subset of mutant *KRAS*-driven lung cancer cells (NCI-H441, H727). Together, our data provide sufficient rationale to test the therapeutic efficacy of an approved MEKi along with simvastatin in a selected subset of *KRAS*-mutated CYP24A1– high lung adenocarcinoma patients in a future clinical trial.

On the contrary, we established that increasing CYP24A1 expression led to increased growth of mutant KRAS lung AC. To determine this phenomenon, we used high-dose calcitriol in *Lsl-Kras^{G12D}* mice. Increased growth of tumors (Fig. 5) was associated with calcitriol-induced up-regulation of CYP24A1. Similar observation was noted specifically in mutant *KRAS*-driven cell lines treated with calcitriol following CYP24A1 up-regulation (Fig. 5*D*). These observations provided a probable molecular explanation of the suboptimal response noted in our

clinical trial (39). Current mechanistic data led us to hypothesize that besides enzymatic activity, the physical presence of CYP24A1 may be critical for promoting tumor cell proliferation. Identification of D-boxes in CYP24A1 helped us identify a direct role of this protein in cell cycle regulation via regulating APC/C complex. Additionally, we identified agents that can physically destabilize CYP24A1 protein to inhibit tumor growth. Furthermore, we noted higher expression of *CYP24A1* Iso2, which lacks exon 10 and the catalytic cysteine, in lung adenocarcinoma samples, supporting functional distinction between normal vitamin D catalytic function from its oncogenic/growth-promoting activity.

We also recognize certain limitations of our study; first, our study does not provide any mechanistic insight why CYP24A1 behaves as a pseudo-substrate like EMI1 and ACM1 as opposed to a true substrate for degradation. In a recent report it was shown that during cell cycle progression, a dual negative feedback switch between CDH1 and EMI1 may be critical in cell cycle commitment; during G_1 phase, EMI1 level is lower because of CDH1-mediated degradation, whereas during progression into S phase with higher CDK2 activity, there is an increase in EMI1 mRNA expression, allowing EMI1-mediated inhibition of CDH1 activity (40). As CYP24A1 levels oscillate during cell cycle progression, future studies may be necessary to understand the interaction between CYP24A1 and CDH1/CDC20 and a possible involvement of posttranslational modifications (*e.g.* phosphorylation) in the process. In our studies using isoform-specific tagged cDNA constructs we noted distinct bands; the cause of such mobility shift is yet unknown. Second, we noted overexpression of D#2 mutant of CYP24A1 causing accumulation of p21, which may be related to an enhanced CDC20 degradation by the hyperactivated CDH1. p21 has been implicated in mitochondrial biogenesis, where loss of p21 causes aberrant increase in mitochondrial mass. Further investigations may help establish these connections. Finally, *in vivo* therapeutic efficacy of dual treatments with a MEKi and simvastatin remains to be tested in preclinical lung tumor models, which can identify lung cancer subsets (mutant *KRAS* with CYP24A1 high), where such a strategy may provide better therapeutic advantage prior to proceeding to the clinic.

Experimental procedures

Materials

Antibody to CYP24A1 (cat. no. ab203308) was obtained from Abcam. Various cyclin antibodies, including cyclin E, A, and B1, were purchased from Millipore. CDC20, SKP2, DRP1, and GAPDH antibodies were from Santa Cruz Biotechnology, and V5 and HA antibodies were purchased from Invitrogen. V5 and c-Myc agarose beads (cat. no. A-7345 and cat. no. 631208, respectively) were from Millipore-Sigma and Clontech, respectively.

Methods

Cell culture

Human embryonic kidney (HEK293) cells and lung adenocarcinoma A549, NCI-H441, and NCI-H727 were acquired from the American Type Culture Collection. HEK293 cells were grown in DMEM and A549, H441, and H727 cells were grown in RPMI 1640 medium supplemented with 10% cosmic calf serum. Mutant Kras (G12D)-inducible primary mouse pancreatic cancer cell lines (4292 and 9805) were cultured in DMEM with 10% Tet FBS and mutant KRAS expression was induced with addition of doxycycline (1 μg/ml) as and when necessary. A day prior to experiments, cells were trypsinized and plated onto cell culture dishes.

Site-directed mutagenesis

For overexpression of CYP24A1, pLX304 vector with human *CYP24A1* with in-frame–fused V5-tag was purchased from DNASU (ASU Biodesign Institute, Arizona State University, Tempe AZ) and control vector (pLX304) was obtained from Addgene (Cambridge, MA). We have also used pCMV6-CYP24A1 (Myc-DDK tagged) isoform 2 from OriGene Technologies (cat. no. RC225738). To insert site-specific mutation, we have used QuikChange mutagenesis kit from Stratagene and used according to manufacturer's protocol. To confirm mutations, isolated plasmids were sequenced at the University of Michigan DNA sequencing core and analyzed.

Stable transfection

SK-Lu1 cells were plated in 12-well plate at the density of 50,000 cells/well and incubated overnight. Next day plasmids were transfected using FuGENE 6 Transfection Reagent (Promega, Madison, WI) according to the manufacture's protocol. 48 h after transfection cells were subjected to selection using blasticidin (10 μg/ml).

Transient transfection

HEK293 cells were used from all transient transfection studies using calcium phosphate method as described previously. Briefly, 150,000 cells were plated in 3.5-cm tissue culture dishes in serum containing medium and incubated overnight. Next day, cells were treated with chloroquine 1 h prior to addition of DNA-calcium phosphate complex. Complexes were incubated for 6 h prior to removal and replacement with complete growth medium. Cells were then left for 48 h (unless mentioned otherwise) prior to cell lysis and protein isolation.

Immunoblotting

For cells lysis we have used a lysis buffer containing 50 mM HEPES.KOH, 150 mM NaCl, 1 mM EDTA, 2.5 mM EGTA, 1 mM NEM, 1 mM NaF, 100 μM sodium orthovandate, 10% glycerol, 10 mM β-glycerophosphate, 20 mM ammonium molybdate, 0.1% Nonidet P-40, and protease inhibitor mixture. All samples were sonicated for complete lysis and centrifuged to remove debris, and supernatants were transferred to a fresh tube. Protein estimation was performed using the Bradford method. A 4× loading buffer containing 250 mM Tris (pH 6.8), 40% glycerol, 4% SDS, 12.5 mM EDTA, 10% β-mercaptoethanol, and 0.08% bromphenol blue was added to each sample and boiled for 5 min before snap freezing. Equal amounts (μg) of proteins from each sample were then loaded to a 4–12% pre-cast Bis-Tris gel (Invitrogen). Proteins were then transferred to a PVDF membrane, blocked with 5% BSA with 1% normal goat serum in 1× Tris-buffered saline (TBS) and 0.05% Tween 20 at room

temperature for an hour. Membranes were incubated with 1 μg/ml primary antibody overnight at 4 °C. Next day membranes were washed in 1× TBS with 0.05% Tween 20 (TBST) and incubated with HRP-conjugated secondary antibody for an hour at room temperature. Following, membranes were washed three additional times with TBST, and bound antibody was detected using an enhanced chemiluminescence agent.

Co-immunoprecipitation

For such studies 500 μg of total protein lysates were used, which were normalized to the same volume. 1 μg of primary antibody was then added to each sample and incubated overnight at 4 °C. Next day, Sepharose Protein A/G beads were washed three to four times using TBST, re-suspended and 100 ml of the bead suspension was added to each sample and incubated for 45 min at 4 °C in a rotator. Beads were then washed three times with lysis buffer, re-suspended in 1× sample loading buffer and boiled for 5 min to release immunoprecipitated proteins. Samples were then subjected to immunoblotting as above using indicated antibodies. For certain studies, we have used either V5- or Myc-tagged agarose beads.

Cell synchronization studies

Cell synchronization studies were performed as described previously. Briefly, we followed a double-thymidine protocol. First, we treated cells with 2 mM thymidine for 18 h, washed once in PBS, and released into fresh media. After 9 h, we added back 2 mM thymidine and further incubated for 15 h. For synchronous progression into early S phase, cells were then released into a fresh medium. Single cell suspensions were fixed using ice-cold 70% ethanol at every 2 h post thymidine-release and subjected to FACS analysis following counterstaining with DAPI (4,6-diamidino-2-phenylindole) for total DNA content. Total cell lysates were also prepared and subjected to immunoblot analyses for checking the cell cycle–regulated expressions of different proteins.

In vitro ubiquitination assay

To obtain semi-purified APC we followed the previously published procedure (41). Briefly, HeLa cells were treated with thymidine (2.5 mM) for 24 h followed by nocodazole (60 ng/ml) for 14 h. Cells were then released from nocodazole to fresh medium for 3 h to reach G_1 phase. To pull down APC complex such synchronized cell lysates were immunoprecipitated with anti-CDC27 antibody at 4 °C overnight. The pulldown protein A/G beads were washed four times with TBS and were aliquoted to different tubes as a source of APC-CDH1. 0, 0.2, 0.5, and 1 μg His-CYP24A were preincubated with the beads at 30 °C for 1 h. Then recombinant E1, E2, ubiquitin, His-Myc-cyclin B (1–102), and energy regeneration mix (ATP, creatine phosphokinase, phosphocreatine) were added to each reaction. The reactions were incubated at 30 °C for 30 min in shaking. The supernatant was collected and mixed with SDS sample buffer and subjected to immunoblotting. Similarly, the beads were also washed with TBS for four times before mixing with SDS sample buffer and subjected to immunoblot analysis.

Maintenance of LSL-Kras^{G12D} mice and tumor induction

All animal experiments were performed according to the University of Michigan Committee on the Use and Care of Animals (UCUCA)–approved protocols (10412-1 and 08646) and conform to their relevant regulatory standards. *LSL-Kras*^{G12D} mice were obtained from National Cancer Repository and crossed with LSL-Rosa26-Luciferase (obtained from The Jackson Laboratory, stock no. 005152) to generate the compound transgenic mice (*LSL-Kras*$^{G12D/+}$; *LSL-Rosa26*$^{Luc/+}$). For genotyping of the WT *Kras* and Cre-recombined *LSL-Kras*^{G12D}, we used three primers: 5′-GTCTTTCCCCAGCACAGTGC, 5′-CTCTTGCCTACGCCACCAGCT, and 5′-AGCTAGCCACCATGGCTTGAGTAAGTCTGCA. For the detection of *LSL-Rosa26*^{Luciferase} allele primer sets of 5′-CGTGATCTGCAACTCCAGTC and 5′-GGAGCGGGAGAAATGGATATG were used.

To induce lung tumors 6- to 8-week-old mice were infected with 3×10^7 plaque-forming unit adenovirus particles encoding Cre recombinase via intranasal inhalation. In this model, within 18 weeks of virus infection lung-specific Kras^{G12D} oncoprotein expression initiated lung adenomas within the lung parenchyma and atypical adenomatous hyperplasia.

Bioluminescence imaging

To observe tumor growth noninvasively, we used bioluminescence imaging. Initially, mice were imaged first after 12 weeks and following that, weekly until we started detecting tumors. For bioluminescence imaging, University of Michigan Molecular Imaging Core facility was used, equipped with PerkinElmer's IVIS 200. Before imaging, mice were injected with D-Luciferin (150 mg/kg) in PBS and anesthetized with isofluorane/air mixture during the imaging period. To detect peak luminescence, serial images were acquired for 20 min with an interval of 2 min and were analyzed.

Micro CT analyses

For micro-CT imaging, a Siemens Invenon System was used with the following parameters: 80 kVp, 500 μA, 400 ms exposure, 360 projections over 360 degrees, and 49.2 mm field of view. For the image analyses, in-house (MATLAB) software with a threshold of −200 Housefield units was used, which determined the tumor volume. For micro-CT, mice were imaged at 2 weeks post calcitriol treatment following tumor detection.

Clonogenic cell survival assay

Clonogenic survival assays were performed following the plating of 250 cells in 35-mm cell culture dishes. A day following plating, cells were either left untreated or treated with different doses of calcitriol/metformin either alone or in combination. 6 to 9 days later, cell colonies formed were fixed (methanol:acetic acid/methanol, 7:1 ratio) and stained with a crystal violet (0.5%, w/v) solution. Colonies were counted using a stereomicroscope and the fraction of cell colonies formed following different treatments were normalized to the survival of the untreated control cells.

Statistical analyses

The Student's *t* test or paired *t* test was used to determine the significance of differences between groups with 95% confidence as the desired level of statistical significance. For protein half-life study calculation, we used the Hill Equation (34), implemented in Prism (GraphPad, San Diego, CA; version 8.0.0), as a sigmoidal function on average protein intensities taken from Western blotting images collected at set time points from treatment initiation from three independent experiments.

Data availability: All data described in the manuscript are located as a part of the main text, figures, and the supporting figures.

Author contributions—W. H., P. R., W. J., Z. W., D. N., G. C., S. G., D. G. B., A. R., N. R., and D. R. data curation; W. H., P. R., W. J., Z. W., D. N., G. C., S. G., A. R., N. R., and D. R. methodology; P. R., W. J., Z. W., D. N., G. C., S. G., T. S. L., A. R., N. R., and D. R. investigation; W. J., D. N., S. G., T. S. L., D. G. B., A. R., N. R., and D. R. formal analysis; D. N., S. G., T. S. L., D. G. B., A. R., N. R., and D. R. writing-original draft; S. G., D. G. B., A. R., N. R., and D. R. project administration; T. S. L., D. G. B., A. R., N. R., and D. R. supervision; A. R., N. R., and D. R. conceptualization; A. R., N. R., and D. R. resources; N. R. and D. R. funding acquisition; D. R. validation.

Acknowledgments—We thank Dr. Marina Pasca di Magliano for kindly providing iKras-inducible primary mouse pancreatic cancer cell lines. We also thank Drs. James Rae, Andrzej Dlugosz, Christine Canman, and David Ferguson for helpful discussion during the study. We thank Steven Kronenberg for graphic assistance.*

References

1. Delbaldo, C., Michiels, S., Rolland, E., Syz, N., Soria, J. C., Le Chevalier, T., and Pignon, J. P. (2007) Second or third additional chemotherapy drug for non-small cell lung cancer in patients with advanced disease. *Cochrane Database Syst. Rev.* **4,** CD004569 CrossRef Medline
2. Gold, K. A., Kim, E. S., Lee, J. J., Wistuba, I. I., Farhangfar, C. J., and Hong, W. K. (2011) The BATTLE to personalize lung cancer prevention through reverse migration. *Cancer Prev. Res.* **4,** 962–972 CrossRef Medline
3. Kim, E. S., Herbst, R. S., Wistuba, I. I., Lee, J. J., Blumenschein, G. R., Jr., Tsao, A., Stewart, D. J., Hicks, M. E., Erasmus, J., Jr., Gupta, S., Alden, C. M., Liu, S., Tang, X., Khuri, F. R., Tran, H. T., *et al.* (2011) The BATTLE trial: Personalizing therapy for lung cancer. *Cancer Discov.* **1,** 44–53 CrossRef Medline
4. Jones, G., Prosser, D. E., and Kaufmann, M. (2012) 25-Hydroxyvitamin D-24-hydroxylase (CYP24A1): Its important role in the degradation of vitamin D. *Arch. Biochem. Biophys.* **523,** 9–18 CrossRef Medline
5. Albertson, D. G. (2003) Profiling breast cancer by array CGH. *Breast Cancer Res. Treat.* **78,** 289–298 CrossRef Medline
6. Mimori, K., Tanaka, Y., Yoshinaga, K., Masuda, T., Yamashita, K., Okamoto, M., Inoue, H., and Mori, M. (2004) Clinical significance of the overexpression of the candidate oncogene CYP24 in esophageal cancer. *Ann. Oncol.* **15,** 236–241 CrossRef
7. Chen, G., Kim, S. H., King, A. N., Zhao, L., Simpson, R. U., Christensen, P. J., Wang, Z., Thomas, D. G., Giordano, T. J., Lin, L., Brenner, D. E., Beer, D. G., and Ramnath, N. (2011) CYP24A1 is an independent prognostic marker of survival in patients with lung adenocarcinoma. *Clin. Cancer Res.* **17,** 817–826 CrossRef Medline
8. Shiratsuchi, H., Wang, Z., Chen, G., Ray, P., Lin, J., Zhang, Z., Zhao, L., Beer, D., Ray, D., and Ramnath, N. (2017) Oncogenic potential of CYP24A1 in lung adenocarcinoma. *J. Thorac. Oncol.* **12,** 269–280 CrossRef Medline
9. Rodriguez, M., and Potter, D. A. (2013) CYP1A1 regulates breast cancer proliferation and survival. *Mol. Cancer Res.* **11,** 780–792 CrossRef Medline
10. Hamasaki, M., Matsumura, S., Satou, A., Takahashi, C., Oda, Y., Higashiura, C., Ishihama, Y., and Toyoshima, F. (2014) Pregnenolone functions in centriole cohesion during mitosis. *Chem. Biol.* **21,** 1707–1721 CrossRef Medline
11. Fang, G., Yu, H., and Kirschner, M. W. (1999) Control of mitotic transitions by the anaphase-promoting complex. *Philosophical transactions of the Royal Society of London. Series B, Biological sciences* **354,** 1583–1590 CrossRef Medline
12. Barford, D. (2011) Structure, function and mechanism of the anaphase promoting complex (APC/C). *Q. Rev. Biophys.* **44,** 153–190 CrossRef Medline
13. Bashir, T., Dorrello, N. V., Amador, V., Guardavaccaro, D., and Pagano, M. (2004) Control of the SCF(Skp2-Cks1) ubiquitin ligase by the APC/C(Cdh1) ubiquitin ligase. *Nature* **428,** 190–193 CrossRef Medline
14. Sivakumar, S., and Gorbsky, G. J. (2015) Spatiotemporal regulation of the anaphase-promoting complex in mitosis. *Nat. Rev. Mol. Cell Biol.* **16,** 82–94 CrossRef Medline
15. Visintin, R., Prinz, S., and Amon, A. (1997) CDC20 and CDH1: A family of substrate-specific activators of APC-dependent proteolysis. *Science* **278,** 460–463 CrossRef Medline
16. Miller, J. J., Summers, M. K., Hansen, D. V., Nachury, M. V., Lehman, N. L., Loktev, A., and Jackson, P. K. (2006) Emi1 stably binds and inhibits the anaphase-promoting complex/cyclosome as a pseudosubstrate inhibitor. *Genes Dev.* **20,** 2410–2420 CrossRef Medline
17. Burton, J. L., and Solomon, M. J. (2007) Mad3p, a pseudosubstrate inhibitor of APCCdc20 in the spindle assembly checkpoint. *Genes Dev.* **21,** 655–667 CrossRef Medline
18. He, J., Chao, W. C., Zhang, Z., Yang, J., Cronin, N., and Barford, D. (2013) Insights into degron recognition by APC/C coactivators from the structure of an Acm1-Cdh1 complex. *Mol. Cell* **50,** 649–660 CrossRef Medline
19. Patel, V., Liaw, B., and Oh, W. (2018) The role of ketoconazole in current prostate cancer care. *Nat. Rev. Urol.* **15,** 643–651 CrossRef Medline
20. Annalora, A. J., Marcus, C. B., and Iversen, P. L. (2017) Alternative splicing in the cytochrome P450 superfamily expands protein diversity to augment gene function and redirect human drug metabolism. *Drug Metab. Dispos.* **45,** 375–389 CrossRef Medline
21. Muindi, J. R., Nganga, A., Engler, K. L., Coignet, L. J., Johnson, C. S., and Trump, D. L. (2007) CYP24 splicing variants are associated with different patterns of constitutive and calcitriol-inducible CYP24 activity in human prostate cancer cell lines. *J. Steroid Biochem. Mol. Biol.* **103,** 334–337 CrossRef Medline
22. Horváth, H. C., Khabir, Z., Nittke, T., Gruber, S., Speer, G., Manhardt, T., Bonner, E., and Kallay, E. (2010) CYP24A1 splice variants—implications for the antitumorigenic actions of 1,25-(OH)2D3 in colorectal cancer. *J. Steroid Biochem. Mol. Biol.* **121,** 76–79 CrossRef Medline
23. Gross, A. M., Kreisberg, J. F., and Ideker, T. (2015) Analysis of matched tumor and normal profiles reveals common transcriptional and epigenetic signals shared across cancer types. *PLoS One* **10,** e0142618 CrossRef Medline
24. Peng, L., Bian, X. W., Li, D. K., Xu, C., Wang, G. M., Xia, Q. Y., and Xiong, Q. (2015) Large-scale RNA-Seq transcriptome analysis of 4043 cancers and 548 normal tissue controls across 12 TCGA cancer types. *Sci. Rep.* **5,** 13413 CrossRef Medline
25. Hyun, S. Y., Sarantuya, B., Lee, H. J., and Jang, Y. J. (2013) APC/C(Cdh1)-dependent degradation of Cdc20 requires a phosphorylation on CRY-box by Polo-like kinase-1 during somatic cell cycle. *Biochem. Biophys. Res. Commun.* **436,** 12–18 CrossRef Medline
26. Amador, V., Ge, S., Santamaría, P. G., Guardavaccaro, D., and Pagano, M. (2007) APC/C(Cdc20) controls the ubiquitin-mediated degradation of p21 in prometaphase. *Mol. Cell* **27,** 462–473 CrossRef Medline
27. Sakaki, T., Yasuda, K., Kittaka, A., Yamamoto, K., and Chen, T. C. (2014) CYP24A1 as a potential target for cancer therapy. *Anti-Cancer Agents Med. Chem.* **14,** 97–108 CrossRef Medline
28. Iizuka-Ohashi, M., Watanabe, M., Sukeno, M., Morita, M., Hoang, N. T. H., Kuchimaru, T., Kizaka-Kondoh, S., Sowa, Y., Sakaguchi, K., Ta-

guchi, T., and Sakai, T. (2018) Blockage of the mevalonate pathway overcomes the apoptotic resistance to MEK inhibitors with suppressing the activation of Akt in cancer cells. *Oncotarget* **9,** 19597–19612 CrossRef Medline

29. Jackson, E. L., Willis, N., Mercer, K., Bronson, R. T., Crowley, D., Montoya, R., Jacks, T., and Tuveson, D. A. (2001) Analysis of lung tumor initiation and progression using conditional expression of oncogenic K-ras. *Genes Dev.* **15,** 3243–3248 CrossRef Medline
30. Bowman, B. M., Sebolt, K. A., Hoff, B. A., Boes, J. L., Daniels, D. L., Heist, K. A., Galbán, C. J., Patel, R. M., Zhang, J., Beer, D. G., Ross, B. D., Rehemtulla, A., and Galbán, S. (2015) Phosphorylation of FADD by the kinase CK1α promotes KRASG12D-induced lung cancer. *Sci. Signal.* **8,** ra9 CrossRef Medline
31. Ostapenko, D., Burton, J. L., Wang, R., and Solomon, M. J. (2008) Pseudosubstrate inhibition of the anaphase-promoting complex by Acm1: Regulation by proteolysis and Cdc28 phosphorylation. *Mol. Cell Biol.* **28,** 4653–4664 CrossRef Medline
32. Di Fiore, B., Davey, N. E., Hagting, A., Izawa, D., Mansfeld, J., Gibson, T. J., and Pines, J. (2015) The ABBA motif binds APC/C activators and is shared by APC/C substrates and regulators. *Dev. Cell* **32,** 358–372 CrossRef Medline
33. Tannour-Louet, M., Lewis, S. K., Louet, J. F., Stewart, J., Addai, J. B., Sahin, A., Vangapandu, H. V., Lewis, A. L., Dittmar, K., Pautler, R. G., Zhang, L., Smith, R. G., and Lamb, D. J. (2014) Increased expression of CYP24A1 correlates with advanced stages of prostate cancer and can cause resistance to vitamin D3-based therapies. *FASEB J.* **28,** 364–372 CrossRef Medline
34. Gadagkar, S. R., and Call, G. B. (2015) Computational tools for fitting the Hill equation to dose-response curves. *J. Pharmacol. Toxicol. Methods* **71,** 68–76 CrossRef Medline
35. Zhang, Q., Kanterewicz, B., Shoemaker, S., Hu, Q., Liu, S., Atwood, K., and Hershberger, P. (2013) Differential response to 1α,25-dihydroxyvitamin D3 (1α,25(OH)2D3) in non-small cell lung cancer cells with distinct oncogene mutations. *J. Steroid Biochem. Mol. Biol.* **136,** 264–270 CrossRef Medline
36. Zou, M., Baitei, E. Y., BinEssa, H. A., Al-Mohanna, F. A., Parhar, R. S., St-Arnaud, R., Kimura, S., Pritchard, C., Alzahrani, A. S., Assiri, A. M., Meyer, B. F., and Shi, Y. (2017) Cyp24a1 attenuation limits progression of Braf(V600E)-induced papillary thyroid cancer cells and sensitizes them to BRAF(V600E) inhibitor PLX4720. *Cancer Res.* **77,** 2161–2172 CrossRef Medline
37. Zou, M., BinHumaid, F. S., Alzahrani, A. S., Baitei, E. Y., Al-Mohanna, F. A., Meyer, B. F., and Shi, Y. (2014) Increased CYP24A1 expression is associated with BRAF(V600E) mutation and advanced stages in papillary thyroid carcinoma. *Clin. Endocrinol.* **81,** 109–116 CrossRef Medline
38. Wan, L., Chen, M., Cao, J., Dai, X., Yin, Q., Zhang, J., Song, S. J., Lu, Y., Liu, J., Inuzuka, H., Katon, J. M., Berry, K., Fung, J., *et al.* (2017) The APC/C E3 ligase complex activator FZR1 restricts BRAF oncogenic function. *Cancer Discov.* **7,** 424–441 CrossRef Medline
39. Ramnath, N., Daignault-Newton, S., Dy, G. K., Muindi, J. R., Adjei, A., Elingrod, V. L., Kalemkerian, G. P., Cease, K. B., Stella, P. J., Brenner, D. E., Troeschel, S., Johnson, C. S., and Trump, D. L. (2013) A phase I/II pharmacokinetic and pharmacogenomic study of calcitriol in combination with cisplatin and docetaxel in advanced non-small-cell lung cancer. *Cancer Chemother. Pharmacol.* **71,** 1173–1182 CrossRef Medline
40. Cappell, S. D., Mark, K. G., Garbett, D., Pack, L. R., Rape, M., and Meyer, T. (2018) EMI1 switches from being a substrate to an inhibitor of APC/C(CDH1) to start the cell cycle. *Nature* **558,** 313–317 CrossRef Medline
41. Tipton, A. R., Tipton, M., Yen, T., and Liu, S. T. (2011) Closed MAD2 (C-MAD2) is selectively incorporated into the mitotic checkpoint complex (MCC). *Cell Cycle* **10,** 3740–3750 CrossRef Medline